Mechatronic Kite and Camera Rig to Rapidly Acquire, Process, and Distribute Aerial Images

Paul Y. Oh and William E. Green

***Abstract*—Aerial images are challenging to acquire in times of a disaster. Conventional aircraft may not be able to takeoff and land due to crippled runways and airstrips. Time is often critical and delays incurred from scheduling a satellite fly-by may frustrate mitigation efforts. A system that can be easily transported to the disaster site and rapidly deployed would be an attractive alternative to aircraft and satellites. This paper integrates mechatronics, intelligent sensing, and mechanism synthesis in a teleoperable kite-mounted camera. Such a system is rapidly deployable, easy to fly, affordable, and can fit in a backpack to quickly acquire, process, and distribute aerial images. Image mosaicing, edge detection, three-dimensional reconstruction, and geo-referencing resulting from images acquired by our aerial platform are also presented.**

***Index Terms*—Aerial photographs, aerial robotics, computer vision, kite, situational awareness, surveillance.**

I. Introduction

AERIAL PHOTOS provide important information for emergency personnel in times of disasters. From such photos, one can assess damages, determine the structural integrity of buildings, plan paths from the disaster site to nearby hospitals, and allocate resources. Of particular concern, is the window of vulnerability immediately following a natural disaster or terrorist attack. Each passing hour leads to additional loss of life, and hence, demands that information like aerial images be acquired, processed, and distributed rapidly. Disasters are fluid and highly dynamic, thus posing a number of challenges to the acquisition of aerial photos. First, disasters cripple runways, and hence, limit takeoff and landing by conventional aircraft. Second, satellites provide detailed images, but scheduling a fly-by incurs delays. Third, unmanned aerial vehicles can also capture images, but flying such aircraft demands highly skilled teleoperators. Fourth, a remote controlled aircraft can be employed and although flying is easier it demands the pilot keep an eye on the model. This becomes very difficult when flying at night or in urban environments. The net effect is that in situational awareness, disaster mitigation, and search-and-rescue operations, there is a need for an aerial image acquisition system that's rapidly deployable, easily transportable, and simple to fly.

Aerial robots have the potential to acquire aerial images but today's prototypes have limitations. Lighter-than-air aircraft like blimps [19] can carry a sizable payload but are difficult to control when windy. Blimps and helium cannisters may be backpackable, but one must also factor that inflation times can delay liftoff. Rotary wing aerial robots [7], including helicopters [13], [16] can also acquire aerial images but often require GPS to navigate autonomously. In urban environments, however, buildings and weather conditions can occlude the line-of-sight to satellites and limit the robot's ability to fly autonomously. Non-GPS based navigation includes visual odometry where visual landmarks are used to localize rotary-wing [1] or fixed-wing [4], [12] with computer vision. Altitude Control Altitude Heading, which only requires a position and velocity command, can be used to stably teleoperate miniature helicopters [5]. Key concerns with using rotary wing vehicles are safety and noise. Time pressures and risks to human life demand that current vehicles become more reliable and robust before they are deployed as effective mitigation agents.

Kites fit in backpacks, are deployable in minutes, easy to fly, and affordable. These characteristics are attractive and this paper describes a mechatronic system, called Low Elevation Aerial Photography (*LEAP*), that can airlift a vision system and quickly acquire aerial images. The accompanying ground station leverages wireless Ethernet (802.11b) to quickly distribute images to end-users like command and control, first responders, site commanders, and tactical decision makers. The current design has a 3-m wingspan that can fly in wind speeds as low as 10 mi/h while carrying a 2-kg payload.[1] The design has flown stably in wind speeds as fast as 25 mi/h [6], [10]. The design features a rip-proof sail, carbon fiber rods and rope having tensile properties that suggest the kite can fly in wind speeds up to 40 mi/h. The kite can be easily and rapidly flown to a 1000 ft (approximately 70 building stories) even at night. The net effect is a kite and teleoperated camera system that integrates mechanism synthesis, mechatronics, computer vision, and wireless networking to acquire, process, and distribute aerial images. The rest of the paper is structured as follows. Section II presents both the kite's dynamic stability and the camera rig's underlying physics, which enable camera orientation to be regulated despite motions of the kite. Section III presents images that can be typically acquired by our system. Work with such images includes image mosaicing, edge detection, three-dimensional (3-D) reconstruction and geo-location referencing. Section IV concludes with our future disaster mitigation endeavors.

II. *LEAP* Design

Changes in wind speed and direction influence a kite's position and orientation. If the camera is rigidly mounted to the kite, desired fields-of-view become very difficult to control; as the kite

Manuscript received February 6, 2003; revised October 23, 2003. This work was supported by U.S. Army Medical Research Acquisition Activity, Fort Detrick, MD, under Grant DAMD17-03-2-0010.

The authors are with the Mechanical Engineering and Mechanics Department, Drexel University, Philadelphia, PA 19104 USA (e-mail: paul@coe.drexel.edu; weg22@drexel.edu).

Digital Object Identifier 10.1109/TMECH.2004.839039

[1]At 10 mi/h winds, leaves are in motion and lightweight flags extend.

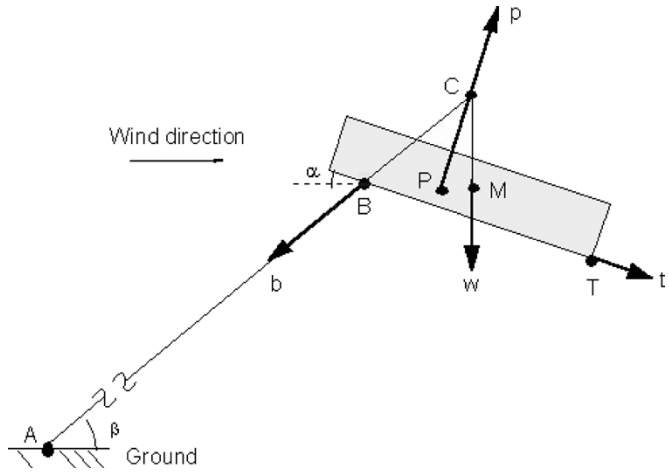

Fig. 1. Simple kite model with forces in balance.

moves, the camera's field-of-view changes. A camera suspended off the kite is even more difficult to control since it can swing and moreover, introduces torques that can destabilize the kite and cause it to crash. Our philosophy in designing systems that move cameras [9], [15] is to formulate the dynamics and leverage them to synthesize mechanisms for visual-servoing. In developing an aerial image acquisition system, the design goal is to construct a linkage that can maintain a constant orientation despite local perturbations. Elliptical pendulums have such a property and are the basis underlying the Picavet linkage, detailed in Section II-C. The dynamic stability of kite flight and camera mechatronics formulated in the next two sections are used to synthesize a camera rig. The net effect is that camera field-of-view can be easily controlled to acquire desired aerial images.

A. Stability Dynamics of Kite Flight

Analyzing the forces acting on a kite can yield wingspan dimensions needed to airlift a desired payload mass. *Ad hoc* oversizing of wingspan or trial-and-error flights is not attractive; larger wingspan kites demand stronger rope and are harder to keep under control in high winds. Essentially, kites remain airborne and in dynamic balance when kite weight w, rope b, and tail t tensions, and wind force p are in balance as shown in Fig. 1. The direction lines of force meet at one common point C called the concurrency point. Ground anchor A, bridle B, and tail T, are fixed points and cannot change. The center of pressure P and mass center M are points within or near the kite. The position of P can theoretically move 25 to 50° along the spine. In practice, however, these are extremes and movement of P is small for angles of attack between 15 to 40° relative to the airstream [11], [20]. The spine in a kite is equivalent to the chord in an airfoil, as such P moves forward as α increases. The amount of movement, however, is more dependent on the viscosity and density of air, which for the simple kite model in Fig. 1 are assumed such that flow about the kite sail remains attached and laminar.

Wind force is proportional to the square of wind speed. Assuming constant kite weight and an unstretchable rope, changes in wind speed will result in a force imbalance, thus prompting kite and/or tail movement. For most kites, the location of the bridle point B is often a small distance away from the kite's sail, and hence, movement about B will be small. Furthermore,

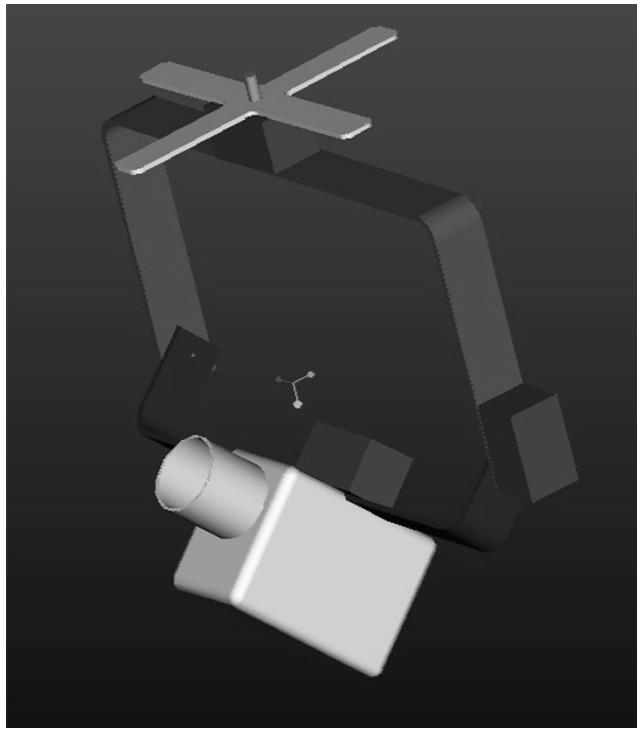

Fig. 2. Pro/E CAD design of the envisioned camera rig.

assuming a light kite and optimal positioning of B, rotation about the bridle point is minimal. In practice, most kites have B located more distant from the sail, making rotation around the bridle point difficult. With tail force typically being small, the only remaining movement possible is about A. Aerodynamically, to compensate for force increase arising from higher wind speed, the kite must decrease angle of attack since we assume no rotation about B. This is a counter-clockwise arching in Fig. 1 and is the marvel of kite flight dynamics; in this nonlinear dynamic balancing act, the kite flies into new states of stability.

Kite wingspan needed to successfully airlift a payload in expected wind speed can be calculated. The underlying physics can be appreciated by assuming a kite sail that is square with side length L. The result is a wind force acting on an effective area of $A = L^2$.

From Bernoulli, lift is proportional to airfoil surface area, air density, and the square of wind speed. It follows that wind force at the center of pressure P (see Fig. 1) is also proportional to the kite's effective area and the square of wind speed V^2. The balance of forces p, w, and b discussed above dictates that $w \approx AV^2$ or

$$V^2 \approx \frac{w}{A}. \tag{1}$$

In other words, wind speed squared is proportional to weight of the kite and payload divided by the area of the kite sail. Independent of wind speed is buoyancy, which dictates a constant mass ratio μ (mass of air displaced versus mass of kite). Kite mass is proportional to its weight w. The displaced air mass, being a volume, must be proportional to another volume, namely L^3. This yields

$$\mu \approx \frac{L^3}{w}. \tag{2}$$

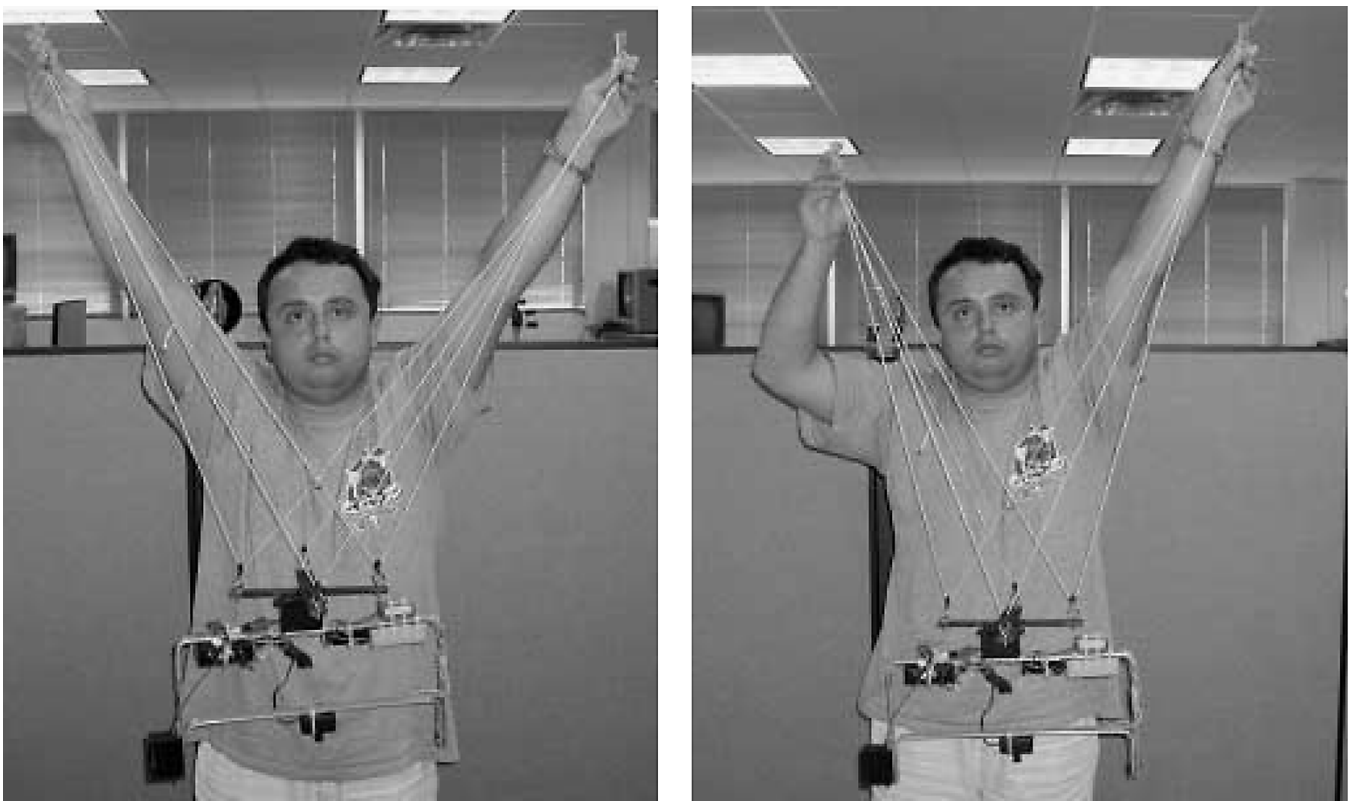

Fig. 3. Left: Picavet initial attitude. Right: attitude is unchanged despite pendulum sway.

In other words, with a constant mass ratio, upscaling a stable kite to a side length $L' = XL$ where $X > 1$ will result in a new effective area $A' = X^2A$ and from (2), the new kite weight is $w' = X^3w$. From (1), the new wind speed required to be airborne is $V' = VX^{1/2}$. Such upscaling results in weight growing with volume, loss of stability at higher wind speeds, and more wind is needed to remain airborne.

Alternatively, changing mass ratio, a heavier kite for instance, can increase stability. For a specific wind speed V, an upscaling with $L' = XL$ where $X > 1$ will increase effective area $A' = X^2A$ and from (1) results in $(w'/A') = (w/A)$. Thus kite weight grows with area and yields $\mu' = X\mu$.

The net effect is that given a kite that flies stably at a specific wind speed or defined mass ratio, the necessary changes in wingspan can be calculated.

B. Camera Rig Mechatronics

The envisioned camera rig, Fig. 2, was modeled in Pro Engineer (Pro/E), a popular CAD package. The rig would suspend off the kite's rope and have two RC (radio-controlled) servos to pan and tilt a lightweight wireless camera. These servos permit a person on the ground to remotely control camera orientation with respect to the rig. Live video is wirelessly transmitted to a ground-based receiver which allows the camera's field-of-view to be monitored and recorded on a handheld camcorder. Video would be uploaded to a laptop equipped with an IEEE 1394 firewire interface and IEEE 802.11b wireless ethernet card. This allows the laptop to web stream video and/or upload image stills to remotely located web servers. The net effect is a portable system that gives users with Internet access, an "eye" in the sky. *LEAP* can rapidly acquire, process, and distribute aerial images. The Pro/E model was constructed to help rapidly develop a physical prototype. Forces and torques on the Picavet (derived in the next section) are related to its weight, wind speed and kite size. By introducing these motion dynamics into the CAD model, design tradeoffs, like smaller wingspan but faster wind speed, can be quickly assessed. Such a procedure revealed that a 3-m wing span would air lift a 1.5-kg camera rig in wind speeds ranging from 10 to 30 mi/h.

C. Picavet

The rig's RC servos permit fixating the kite-mounted camera. When the rig is tied to the kite's rope, it will sway when the kite moves in the wind. This swaying makes radio-controlling camera orientation to fixate on ground subjects very difficult. Swaying also introduces a torque which can destabilize the kite and cause it to crash. A mechanism based on an elliptical pendulum, known as a Picavet linkage, can be kinematically synthesized to keep the camera rig attitude constant despite changes in kite orientation.

The net effect is that the camera's image plane can be stabilized, and therefore controlled. The Picavet linkage, Fig. 3, consists of a crossbar utilizing four pulleys on each end as attachment points, one continuous rope, two brackets that are fixed to the kite line and a ring used to constrain the two innermost lines as they cross.

As the kite increases/decreases its angle-of-attack and assuming friction can be neglected, the rope will glide effortlessly through the pulleys on the cross, keeping the rig undisturbed. As such, because there is no net torque on the rig, the kite is in dynamic equilibruim. Fig. 3 is used to simulate a change in kite

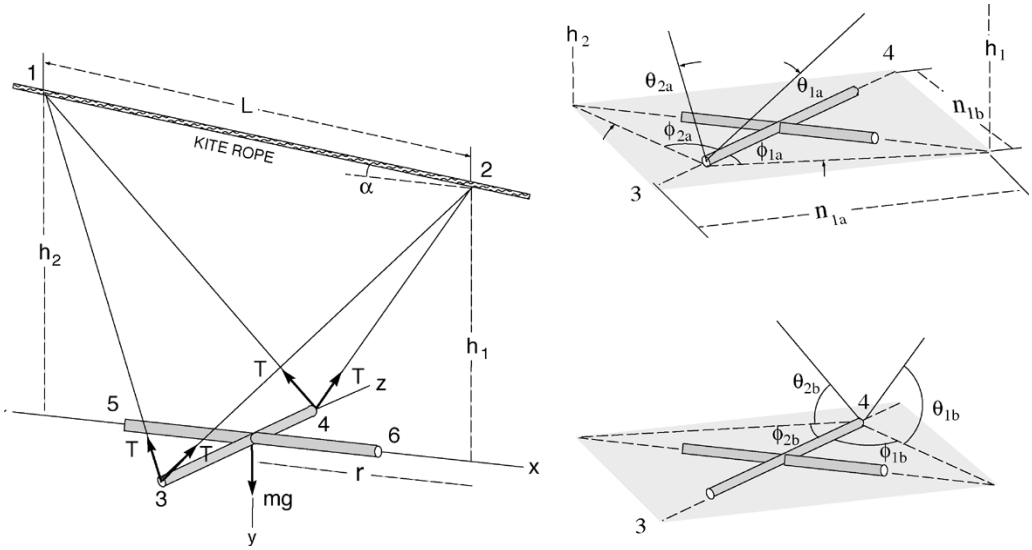

Fig. 4. Picavet free body diagram. A single rope loops through pulleys 1 and 2 on the kite rope and pulleys 3 through 6 on the crossbar. For clarity, tension forces T acting on the Picavet crossbar at pulleys 3 and 4 are shown (left). A symmetrical set of forces T exists on the crossbar at pulleys 5 and 6. Relevant angles at pulley 3 (top right) and pulley 4 (bottom right) are given. Grayshaded planes were drawn to clearly show where the angles θ and ψ are defined.

orientation. The two points, held by hand in the photo, clip onto the kite's rope. The left photo shows the Picavet's initial orientation with the rig's attitude being parallel to the ground. The right photo depicts that while there is a change in the kite's orientation (as simulated by changes in hand position) the rig's orientation remains parallel to the ground. Furthermore, if the linkage is initially oriented such that the crossbar is at some angle relative to the ground, the camera rig maintains this original orientation.

Fig. 4 depicts a small body force diagram. All tensions are the same because a single rope loops through all pulleys at the crossbar tie-points. The *x* axis goes through the midpoint of the bar and is perpendicular to it. This demands that ϕ_{1a}, ϕ_{1b}, θ_{1a} and θ_{1b} are all less than 90°. Furthermore

$$\tan\phi_{1a} = \tan\phi_{1b} = \frac{r}{\frac{l_{\text{bar}}}{2}}. \tag{3}$$

So $\tan\phi_{1a} = \tan\phi_{1b}$ and because ϕ_{1a} and ϕ_{1b} are less than 90° we have $\phi_{1a} = \phi_{1b}$. Thus $n_{1a} = n_{1b}$ and

$$\tan\theta_{1a} = \frac{h_1}{n_{1a}} \quad \text{and} \quad \tan\theta_{1b} = \frac{h_1}{n_{1b}}. \tag{4}$$

Hence, $\tan\theta_{1a} = \tan\theta_{1b}$ and since θ_{1a} and θ_{1b} are both less than 90°, we have $\theta_{1a} = \theta_{1b}$. Similarly

$$\phi_{2a} = \phi_{2b} \tag{5}$$

$$\theta_{2a} = \theta_{2b}. \tag{6}$$

Proving the sum of the moments about the center of mass of the bar are equal to zero will prove that it remains in its initial position. The moments about the *y* axis can be disregarded because rotation about the *y* axis will not change the bar's orientation relative to the ground. $\sum M_x = 0$ can be shown. Assuming counterclockwise as the positive direction yields

$$\sum M_x = \begin{cases} -\frac{1}{2}Tl_{\text{bar}}\sin\theta_{1a} - \frac{1}{2}Tl_{\text{bar}}\sin\theta_{2a} \\ +\frac{1}{2}Tl_{\text{bar}}\sin\theta_{1b} + \frac{1}{2}Tl_{\text{bar}}\sin\theta_{2b}. \end{cases} \tag{7}$$

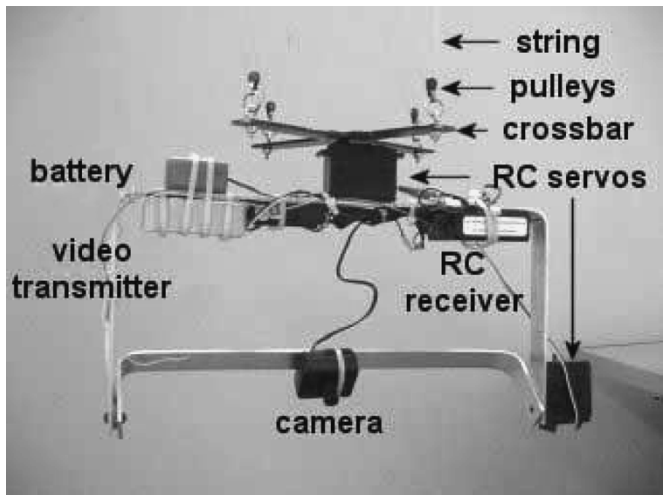

Fig. 5. Mechatronic camera rig designed with RC servos, 1/4 mi range 4-mm-lens focal length video transmitter and battery pack. Pan and tilt range are both ±30°.

Assuming that the rope is attached at the centerline of the bar, the perpendicular distance between the bar and any resulting horizontal tension forces will be zero. This makes the moment about the z axis zero so $\sum M_z = 0$.

A prototype Picavet camera rig was constructed as shown in Fig. 5. The rig's total mass was 1.2 kg and is equipped with a 2.4 GHz wireless camera, two RC servos and battery pack.

III. Image Acquisition and Processing Results

The kite and the camera rig shown in Fig. 5 were flown to approximately 700 ft in urban and rural areas. Ten minutes of video were recorded and Fig. 6 shows image stills. The left image resulted from flying on campus in urban West Philadelphia. The right image resulted from flying in Valley Forge National Park, a rural area approximately 20 mi outside the city. As can be seen, such images provide rich detail. While commercial aircraft can capture such detail, the resulting aerial photographs are expensive; aircraft are restricted from flying at low

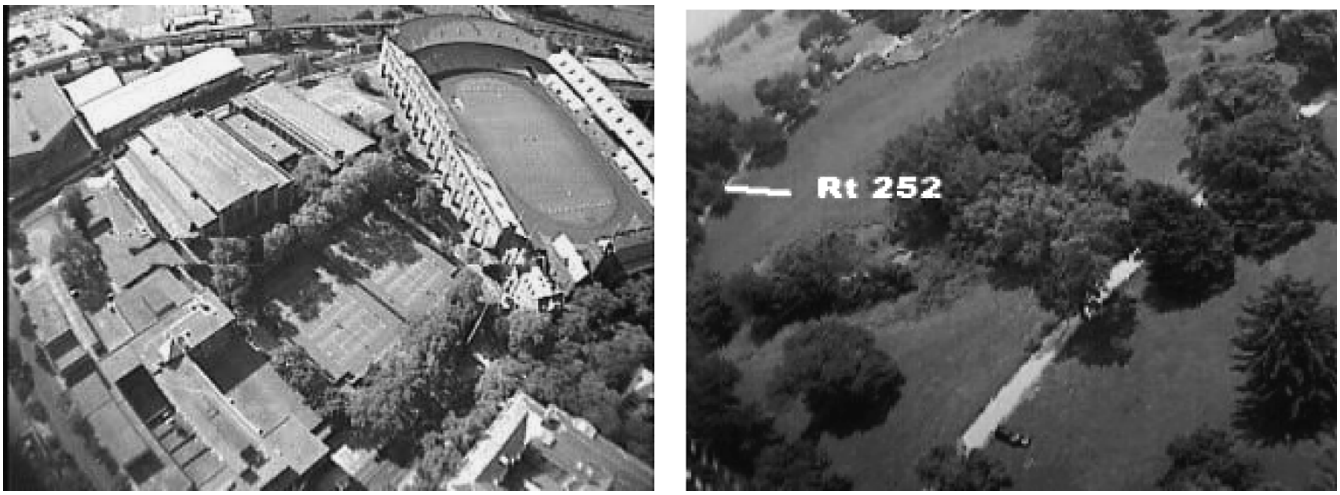

Fig. 6. Sample aerial images acquired at 700 ft with the camera rig shown in Fig. 5. The left image was captured on-campus in University City in Philadelphia. The right image was acquired while flying in Valley Forge National Park 20 mi outside the city. Text highlighting the highway was added.

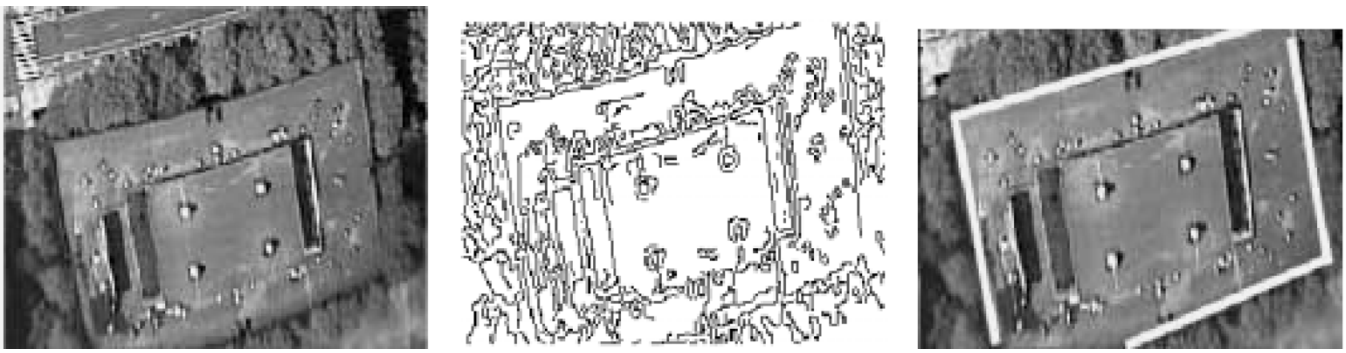

Fig. 7. A raw aerial image (left) can be processed with a Canny edge detector (center) and Hough transform to detect a roof's perimeter (right).

altitudes, and hence, use expensive equipment like fast shutter power zoom cameras with active stabilization mechanisms. The kite and camera rig provides image detail by flying at low altitude but delivers a narrow field-of-view, approximately 4×4 city blocks from 700 ft. Also, within the designed flight regime of 10 to 20 mi/h wind speed, small irregularities in wind speed and direction are absorbed by the kite such that the center of pressure does not move.

Raw aerial images can appear extremely convoluted to the untrained eye. Image processing can enhance features and help end users, like site commanders and decision makers, interpret visual data. For example, Canny edge detection [2] and Hough transforms were applied to an aerial photo to automatically identify the roof's perimeter (see Fig. 7). As a result, several well-known computer vision techniques were executed to demonstrate the processing of aerial imagery. For example, mosaicking and 3-D reconstruction were performed off-line by using image stills extracted from the 10 min of video that was captured. Results of such techniques are presented next.

A. Image Mosaicing

Image mosaicing is the process of stitching several images together to yield a single larger image. Because a stationary camera typically has a field-of-view of only 50°, a moving camera can be used to capture more slices of an area. These multiple image slices can be mosaiced together to give an entire view of a scene. For example, in Fig. 8, the surrounding three images were acquired by the aforementioned mechatronic camera rig, and used to generate the resulting mosaic (center). Looking at a single mosaiced image rather than six or seven separate images showing equivalent information will be time efficient. In Szeliski's original method of mosaicing, the user identifies and relates common points among two or more images [17]. Any two common points are related to each other by a translation and a rotation. Four common points, two in each image, are needed to generate the transformation matrix, M. Once, the transformation matrix is known, the points in the original images, u, can be mapped algorithmically to the mosaiced image, u', by the relation $u' = Mu$. and implemented at Matlab.

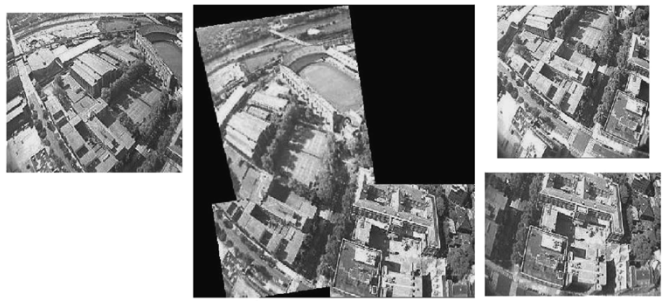

Fig. 8. Image mosaic created from aerial images acquired by *LEAP*.

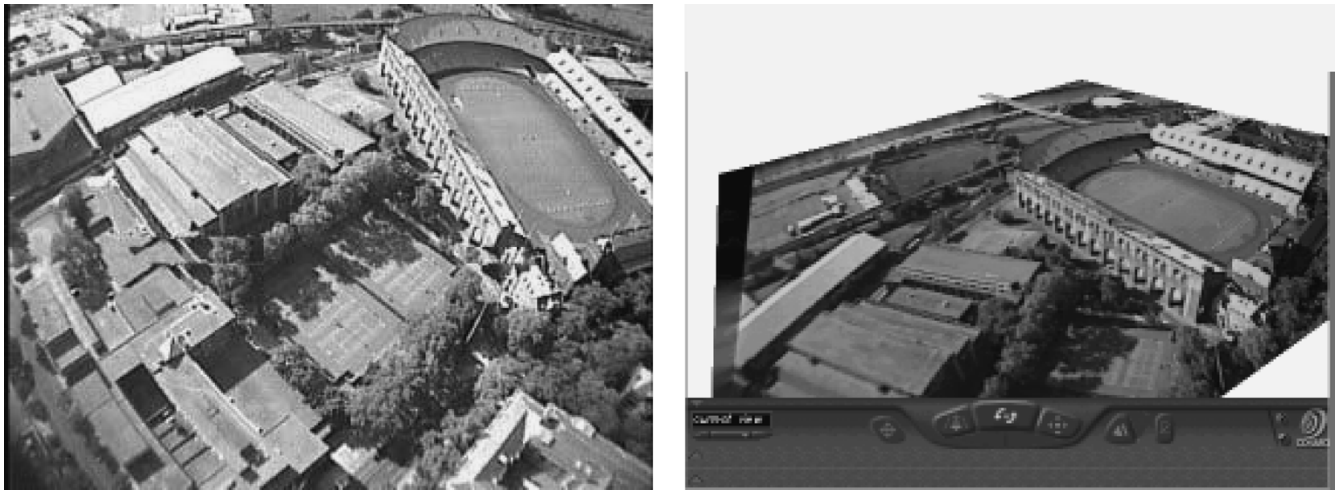

Fig. 9. Aerial photo of urban ground scene at 1000 ft (left) and 3-D reconstructed model (right).

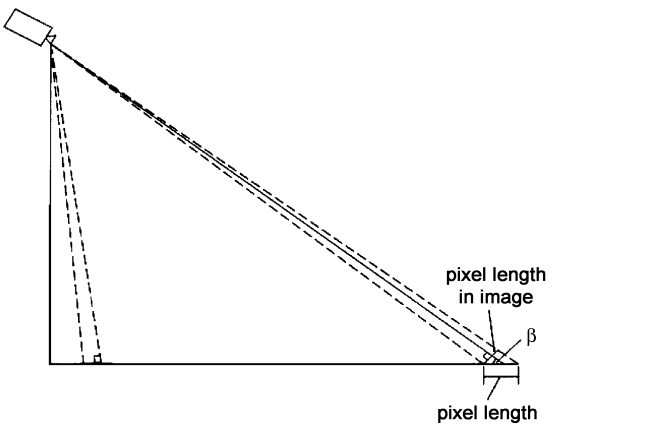

Fig. 10. Pixel to world space mapping calculations.

B. 3-D Reconstruction

A two-dimensional (2-D) image offers a limited range of capabilities to search-and-rescue teams. They cannot go beyond cropping and resizing a specific area to get a close up view. However, gathering information about several areas could be arduous and time consuming. Fig. 9 (left) depicts a 2-D aerial photo. It can be seen that it is virtually impossible to interact with this image to rotate around and look behind buildings.

Three-dimensional reconstruction is a technique that generates 3-D models from 2-D images [8], [14], [18]. Fig. 9 (right) shows the 3-D reconstructed model of the image still (left) using a commercial version of Facade [3] called Canoma. This package generates virtual models by prompting the user to specify lines planes and triangles that belong to a building's edges, walls, and roofs. This technique is much faster than an automated process. For example, it took one lab member less than 30 min to reconstruct the model in Fig. 9. Once created, the user can rotate, pan, and zoom the 3-D model via a VRML-enabled web browser.[2]

C. Geo-Location Referencing

Size perception is greatly diminished when looking at an aerial photograph. There is no scale conveniently displayed in the bottom corner of the image like on a map. This makes the mundane task of estimating distances more complex. It would be very useful to site commanders to be able to accurately gauge distances in order to, for example, ascertain whether an ambulance can fit through a blocked road.

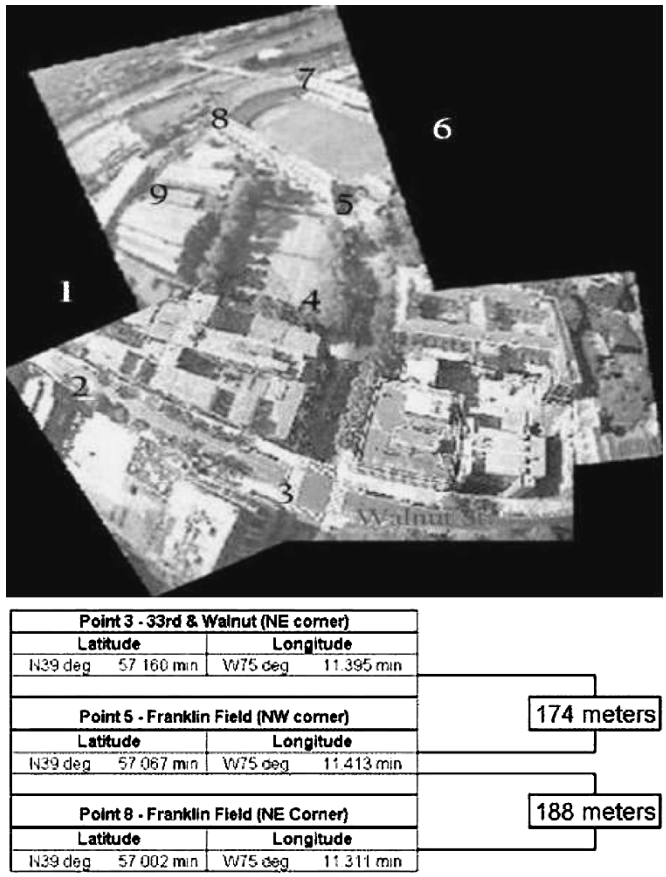

Fig. 11. Image geo-referenced with longitude/latitude coordinates.

Integrating the processed images with GPS coordinates that reference landmarks in the image, Fig. 11, would give a better approximation of distance. A pixel-to-meter ratio can be found by relating the GPS measurements to the corresponding pixel lengths in the image. The longitudinal and lateral coordinates

[2]http://prism.mem.drexel.edu/projects/kite/index.html hosts the VRML model where one can virtually fly through an urban area near West Philadelphia.

were collected from nine known landmarks shown in the Fig. 11. These were then mapped to the mosaiced image. However, this method will not yield a pixel-to-meter ratio that is homogeneous throughout an entire image. As seen from Fig. 10, the error in estimating the perceived pixel length in comparison with the actual pixel length is going to increase as you move further away from the camera. The relationship that will compensate for this error is

$$\text{Pixel Length} = \frac{\text{Pixel Length in Image}}{\sin\beta} \tag{8}$$

where β is the flying angle. GPS-to-pixel mapping can then be accomplished with a few referenced points in the image leveraging search and rescue's ability to accurately judge distances throughout the image.

IV. Conclusion

In time-critical situations there are challenges to acquiring aerial images with conventional aircraft, satellites, unmanned aerial vehicles, and radio-controlled or robotic blimps, airplanes, and helicopters. Challenges like crippled runways, damaged roads, delays, transportability, deployment delays, user difficulty, and expense must be all considered when designing a system to augment mitigation efforts. Presented in this paper is *LEAP*, a system that overcomes these challenges. *LEAP* is a mechatronic teleoperated kite retrofitted with a camera rig and a ground-based monitoring and network system that permits rapid acquisition, processing and distribution of aerial images. The off-the-shelf kite presented in the paper is man-backpackable, affordable, easy to deploy even at night and can quickly reach flying altitudes of 1000 ft or greater.

The flight mechanics and dynamic balance that relate payload weight, wind speed, and kite wingspan were presented. In addition, the attitude-regulating ability of the Picavet camera rig was analyzed. Elliptical pendulum literature is widespread but to the best of our knowledge, this paper is the first to present the Picavet's underlying mathematics. The intent of this was to assist researchers, interested in airborne instrumentation, in assembling their own kite-based rig. The image mosaicing, edge-detection 3-D reconstruction and geo-referencing results leveraging the acquired aerial images illustrate some potential tasks. The marriage of mechatronics, intelligent sensing, and mechanism synthesis follows our philosophy of holistically designing computer vision systems. This resulted in an affordable, rapidly deployable, transportable, and easy to fly system. In applying *LEAP* to disaster mitigation, we are currently investigating ingress/egress route generation. We hope to reference *LEAPs* aerial images with private and public geospatial databases to automate driving directions for emergency medical teams moving between the site and hospitals. The databases would propose directions and *LEAPs* real-time aerial images would assess if a particular road is blocked (by fire trucks for instance) or is damaged. Another research direction is to mount altimeters, encoders and possibly GPS on the camera rig to perform visually servoed tracking. Such pose data, along with live video, can be wirelessly transmitted to the ground station laptop. This would eliminate teleoperation, which can be tedious, and enable computer controlled camera servoing. Several key issues that must be considered beforehand are handling any lighting changes and degraded communications between the airborne rig and ground computer, and 802.11b dropouts between the ground computer and lab server.

References

[1] O. Amidi, T. Kanade, and K. Fujita, "A visual odometer for autonomous helicopter flight," *Robot. Auto. Syst.*, vol. 28, no. 28, pp. 185–193, 1999.

[2] J. Canny, "A computational approach to edge detection," *IEEE Trans. Pattern Anal. Machine Intell.*, vol. PAMI-8, pp. 679–698, Nov. 1986.

[3] P. Debevec, C. J. Taylor, and J. Malik, "Modeling and rendering architecture from photographs: a hybrid geometry-and-image-based approach," in *Proc. SIGGRAPH Computer Graphics*, New Orleans, LA, Aug. 1996, pp. 11–20.

[4] S. M. Ettinger, M. C. Nechyba, P. Ifju, and M. Waszak, "Vision-guided flight stability and control for micro air vehicles," in *IEEE/RSJ Int. Conf. Robots and Systems*, Lausanne, Switzerland, Oct. 2002, pp. 2134–2140.

[5] V. Gavrilets, I. Martinos, B. Mettler, and E. Feron, "Control logic for automated aerobatic flight of miniature helicopter," in *AIAA Guidance, Navigation, and Control Conf.*, Monterey, CA, Aug. 2002.

[6] W. E. Green and P. Y. Oh, "An aerial vision platform for acquiring situational awareness," in *Proc. Int. Conf. Computer, Communication, and Control Technologies*, vol. 5, Orlando, FL, July 2003, pp. 289–295.

[7] T. Hamel, R. Mahony, and A. Chriette, "Visual servo trajectory tracking for a four rotor VTOL aerial vehicle," in *Proc. IEEE Int. Conf. Robotics and Automation*, Washington, DC, 2002, pp. 2781–2786.

[8] L. McMillan, "Acquiring Immersive Virtual Environments With an Uncalibrated Camera," Univ. North Carolina, Chapel Hill, NC, UNC Technical Report TR95-006, 1995.

[9] P. Y. Oh and P. K. Allen, "Visual servoing by partitioning degrees of freedom," *IEEE Trans. Robot. Automat.*, vol. 17, pp. 1–17, Feb. 2001.

[10] P. Y. Oh and W. E. Green, "A kite and teleoperated vision system for acquiring aerial images," in *IEEE Int Conf Robotics and Automation*, Taipei, Taiwan, Sept. 2003, pp. 1404–1409.

[11] R. H. Barnard and D. R. Philpott, *Aircraft Flight*, 2nd ed. Englewood Cliffs, NJ: Prentice-Hall, 1995.

[12] F. Pipitone, B. Kamgar-Parsi, and R. Hartley, "Three dimensional computer vision for micro air vehicles," in *SPIE 15th Aerosense Symp. Conf. Enhanced and Synthetic Vision* , Orlando, FL, Apr. 2001.

[13] C. S. Sharp, O. Shakernia, and S. S. Sastry, "A vision system for landing an unmanned aerial vehicle," in *Proc. IEEE Int. Conf. Robotics and Automation*, Seoul, Korea, 2001, pp. 1720–1727.

[14] S. Soatto, "3-D structure from visual motion: Modeling, representation and observability," *Automatica*, vol. 33, pp. 1287–1312, 1997.

[15] R. Stanciu and P. Y. Oh, "Designing visually servoed tracking to augment camera teleoperators," in *IEEE Conf. Intelligent Robotics and Systems*, Lausanne, Switzerland, Oct. 2002.

[16] S. Saripalli, J. F. Montgomery, and G. Sukhatme, "Vision-based autonomous landing of an unmanned aerial vehicle," in *IEEE Int. Conf. Robotics and Automation (ICRA)*, Washington, DC, 2002, pp. 2799–2804.

[17] R. Szeliski, "Video mosaics for virtual environments," *IEEE Comput. Graph. Appl.*, vol. 16, no. 2, pp. 22–30, 1996.

[18] C. J. Taylor and D. Kriegman, "Structure and motion from line segments in multiple images," *IEEE Trans. Pattern Anal. Machine Intell.*, vol. 17, pp. 1021–1032, Nov. 1995.

[19] H. Zhang and J. P. Ostrowski, "With dynamics: control of an unmanned blimp," in *IEEE Int. Conf. Robotics and Automation*, Detroit, MI, 1999, pp. 618–623.

[20] H. V. Veen, *The Tao of Kiteflying the Dynamics of Tethered Flight*. Randallstown, MD: Aeolus Press, 1996.

Paul Y. Oh received the B.Eng. (Hons.), M.Sc., and Ph.D degrees in mechanical engineering from McGill University, Montreal, QC, Canada, in 1989, Seoul National University, Seoul, Korea, 1992, and Columbia University, New York, 1999.

His research interests include visual-servoing, mechatronics, and aerial robotics. He was a Summer Faculty Fellow at the NASA Jet Propulsion Lab, in 2002, and at the Naval Research Lab in 2003. He is currently an Assistant Professor in the Mechanical Engineering and Mechanics Department, Drexel University, Philadelphia, PA.

Dr. Oh received a Presidential Young Investigator Award from the National Science Foundation CAREER Award for controlling micro air vehicles in near-Earth environments in 2004. Currently, he chairs the IEEE Technical Committee on Aerial Robotics for the IEEE Robotics and Automation Society.

William E. Green received the B.Sc. degree in mechanical engineering from Drexel University, Philadelphia, PA, in 2002, and is currently pursuing a Ph.D in the Mechanical Engineering and Mechanics Program at the same university.

His research interests include aerial robotics, mechatronics, and computer vision.